Operation Altitude Optimization of Solar-Powered Rotary-Wing UAVs for FSO Backhauling

Khadijeh Ali Mahmoodi, Mohammed Elamassie, Murat Uysal

Department of Electrical and Electronics Engineering, Özyeğin University, Istanbul, Turkey, 34794.

E-mails: khadijeh.ali@ozu.edu.tr, mohammed.elamassie@ozyegin.edu.tr, and murat.uysal@ozyegin.edu.tr.

Abstract—Free space optical communication (FSO) has emerged as an alternative backhauling technology. It provides a line-of-sight (LOS) link with a capacity comparable to fiber optics and much higher than those that can be supported by radio counterparts. Rotary-wing unmanned aerial vehicles (UAVs) equipped with FSO terminals can be positioned as a complementary aerial solution to the terrestrial backhaul links in dense areas with high-peak traffic demands. In this paper, we consider a solar-powered rotary-wing UAV equipped with an FSO terminal that provides backhaul link to a ground base station in an urban area. We first quantify the energy consumption and energy harvesting of a rotary-wing solar-powered UAV. Then, we formulate an optimization problem to determine the optimal operation altitude with the goal of maximizing the net energy of UAV while satisfying the LOS requirements critical for the FSO link. Our results show that the selection of operation altitude is highly dependent on the weight of the UAV as well as the size and efficiency of the solar panel.

Index Terms—Free space optical communication, backhauling, UAV.

I. INTRODUCTION

Unmanned aerial vehicles (UAVs) have been increasingly deployed in various applications such as surveillance and monitoring, delivery of supplies, rescue operations, and wireless communications [1]. UAV-based wireless links can be used as alternative or complementary backhaul/access solutions to terrestrial infrastructure taking advantage of UAV's inherent features such as rapid deployment, high mobility, and adaptive altitude [2].

UAVs can be equipped with a radio base station and deployed as an aerial base station providing wireless access to end users [3]–[6]. For example, in [3], optimum three-dimensional (3D) deployment of multiple UAV base stations is investigated with the goal of improving the coverage rate while satisfying the quality-of-service (QoS) requirements of each user. In [4], an aerial base station placement algorithm is proposed to reduce the number of required UAVs to serve a desired coverage area. In [5], optimum UAV trajectory design is investigated to minimize its mission completion time while ensuring that each ground node receives the required information within a given time. In [6], 3D trajectory optimization of multiple UAVs is pursued with the goal of optimizing the coverage while maximizing the sum of QoS requirements of ground users.

In addition to the line of research on UAV-based wireless access discussed above, it is also possible to utilize UAVs as backhaul links to ground base station. While high-altitude platform stations (HAPSs)[1] are useful for backhauling in rural and wide areas [7]–[9], rotary-wing UAVs have the capability of hovering and might be particularly attractive for small cell backhauling. They can be positioned as a complementary solution to the terrestrial backhaul links in dense areas with high-peak traffic demands. For UAV-based backhauling, the operation frequency can be selected from radio frequency (RF) band [10]–[12] or optical band (in particular, infrared) [13]–[16]. In RF-based solutions, either out-of-band or in-band frequencies can be used for backhauling connectivity [17], [18]. While the use of out-of-band frequency avoids interference, it becomes a more costly approach. On the other hand, in in-band backhauling, a robust interference management becomes critical.

Free space optical communication (FSO) has emerged as an alternative backhauling technology. It uses laser transmitters operating at infrared wavelengths and provides a line-of-sight (LOS) link with a capacity comparable to fiber optics and much higher than those that can be supported by RF counterparts. In addition, since they operate in optical spectrum, they are immune to interference. Furthermore, unlike RF backhaul links which require either area or link license for operation, no licensing fee is required. In [13], with the goal of minimizing the capital cost of the FSO-based aerial backhaul network, the problem of minimizing the number of UAVs is investigated. In [14], to improve the energy efficiency of the UAV-based backhaul networks, a hybrid RF-FSO system is proposed with simultaneous harvesting capability. In [15], to improve the energy efficiency of the UAV-based backhaul network, a modulating retro reflector based FSO system is proposed which leads to increase in the manoeuvrability and flight time of UAVs. In [16], solar powered rotary-wing UAVs are considered and the problem of UAV placement in a dense urban environment is investigated to ensure backhaul connectivity. To maximize the harvested energy, the UAVs are placed in sunny spots between the buildings.

In an urban area with many buildings, the operation altitude of a solar-powered UAV plays an important role in the energy efficiency of the aerial backhaul link. It has a significant effect on the endurance of the solar-powered UAV (which can be quantified in terms of net energy defined as the difference between energy consumption and harvesting) as well as the probability of establishing the LOS link. Some earlier works on RF-based UAV backhauling discussed the optimal selection of altitude. For example, in [11], a mathematical model is

[1]Here, we use the term high altitude platform station (HAPS) to describe UAVs that operate at the stratospheric altitude (17-22 km).
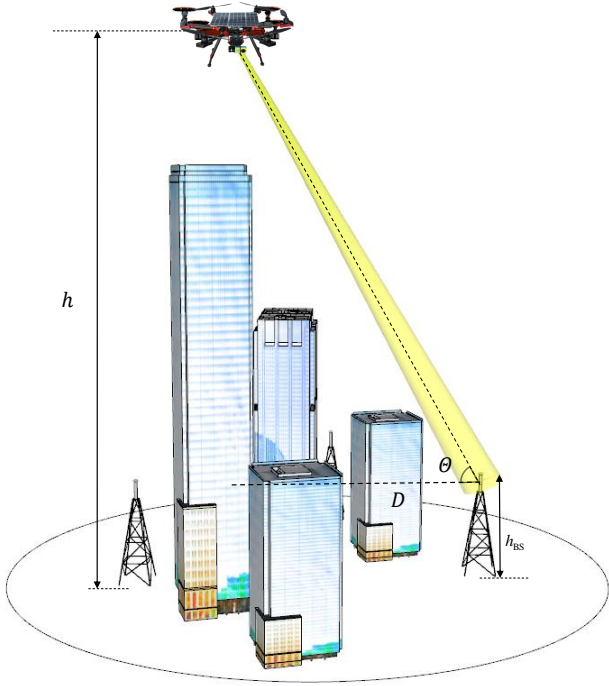
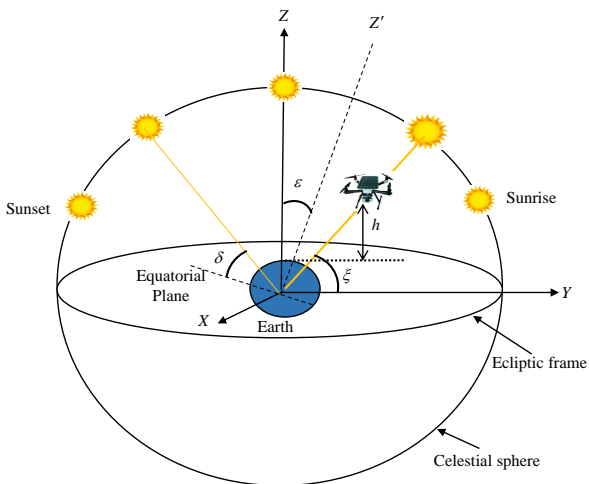Fig. 1. LOS link between the solar-powered rotary-wing UAV and the ground base station in an urban area.

Fig. 2. The location of the UAV with respect to the earth surface and the sun.

presented to determine an optimal altitude with the goal of providing maximum radio coverage on ground assuming in-band frequency of 2 GHz. In [19], optimal altitude is selected to maximize the coverage area for a targeted outage probability.

To the best of our knowledge, the optimal selection of operation altitude for rotary-wing UAVs was not yet investigated in the context of FSO-based backhauling. In this paper, we consider a solar-powered rotary-wing UAV equipped with an FSO terminal that provides backhaul link to a ground base station in an urban area. We first quantify the energy consumption and energy harvesting of a rotary-wing solar-powered UAV. Then, we formulate an optimization problem to determine the optimal operation altitude with the goal of maximizing the net energy of UAV while satisfying the LOS requirements critical for the FSO link.

The rest of the paper is organized as follows: In Section II, we present the system model including the LOS link model, energy harvesting, and energy consumption models. In Section III, we formulate the altitude optimization problem. In Section IV, we provide numerical results and discussions on the performance. We finally conclude in Section V.

II. SYSTEM MODEL

We consider an urban area in cellular networks where a solar-powered rotary-wing UAV provides FSO-based backhaul connectivity to a ground base station as shown in Fig. 1. Due to the small divergence angle of a laser transmitter, this requires the establishment of a LOS link between the UAV and the base station. Here, h_{BS} denotes the height of receiving unit (located on the top of the base station) from the ground, and h is the operation altitude of the UAV. Θ and D denote, respectively, the elevation angle and horizontal distance between the UAV and the base station.

In the urban area scenario under consideration, the tall buildings might obstruct the FSO links which require LOS availability. The probability distribution function (PDF) of the LOS link is given by [11]

$$
\begin{aligned}
& P_{\text{LOS}}\left(\alpha, \beta, D, h, h_{\text{BS}}\right) \\
& = \prod_{k=0}^{\lfloor D\sqrt{\alpha\beta}\rfloor-1}\left[1-\exp\left(-\frac{1}{2\mho^2}\left[h-\frac{\left(k+\frac{1}{2}\right)\left(h-h_{\text{BS}}\right)}{\lfloor D\sqrt{\alpha\beta}\rfloor}\right]^2\right)\right],
\end{aligned}
\tag{1}
$$

where $\lfloor\cdot\rfloor$ is the floor function that maps the inner argument to the maximum integer that is smaller than or equal to it, i.e., $\lfloor x\rfloor = \max\left(m\in\mathbb{R}\,|\,m\leqslant x\right)$, α is a dimensionless unit representing the ratio of built-up area to the total area, and β is the average number of buildings per km^2. In (1), $\mho$ is a scaling parameter that describes the buildings' heights distribution. In [20], the PDF of building height distribution (H) is given by

$$
f_H\left(H\right) = \left(\frac{H}{\mho^2}\right)\exp\left(-\frac{H^2}{2\mho^2}\right).
\tag{2}
$$

The mean of buildings' heights is therefore $\mu_{\text{H}} = E\left[H\right]$, where $E\left[\cdot\right]$ denotes the expectation operator. The scaling parameter can then be defined in terms of the mean as $\mho = \mu_{\text{H}}\sqrt{2/\pi}$.

A. Energy Harvesting Model

As illustrated in Fig. 2, we consider a solar-powered rotary-wing UAV. Let η_{sc} and A_{s} respectively denote the efficiency and the area of the solar panel attached to the UAV. If the airborne duration in hovering status is T hours, the total harvested energy (in Watt-hour^2) is given by [21]

$$
E_{\text{h}} = \int_{t=t_{\text{start}}}^{t_{\text{start}}+T}\psi A_{\text{s}}\eta_{\text{sc}}G_{\text{in}}\left(t\right)dt,
\tag{3}
$$

where t_{start} is the start time of the flight. In (3), $G_{\text{in}}\left(t\right)$ is the instantaneous solar intensity and given by [21]

---

[2]One Watt-hour is equal to 1 Watt of power harvested for 1 hour.

$$G_{\text{in}}(t)$$
$$= \begin{cases} G_{\text{m}} \sin\left(\frac{2\xi_{\text{m}}}{\tau}(t - t_{\text{sunrise}})\right), & t_{\text{sunrise}} < t < 12 \\ G_{\text{m}} \sin\left(\left(2\xi_{\text{m}} - \frac{2\xi_{\text{m}}}{\tau}(t - t_{\text{sunset}})\right)\right), & 12 < t < t_{\text{sunset}} \end{cases}$$
$$(4)$$

where G_{m} is the maximum instantaneous radiation intensity at solar noon (See Appendix for the calculation), ξ_{m} is the maximum elevation angle of the sun, τ is the daylight duration in hours, $t_{\text{sunrise}} = 12 - \tau/2$ is the time when the sun rises, and $t_{\text{sunset}} = 12 + \tau/2$ is the time when the sun sets. In (3), ψ is the atmospheric transmittance, which varies with respect to altitude and is calculated by [22]

$$\psi = 0.8978 - 0.2804 \exp\left(-\frac{h}{3500}\right). \quad (5)$$

Assume that the UAV becomes airborne $T/2$ hours before solar noon[3], i.e., $t_{\text{start}} = 12 - T/2$. By substituting (4) in (3) and solving the resulting integral, we find the harvested energy as (6). The overall input energy of the UAV can be then written as

$$E_{\text{in}} = E_{\text{h}} + E_{\text{b}}, \quad (7)$$

where E_{b} is the initial battery capacity.

B. Energy Consumption Model

The energy consumption of a rotary-wing UAV in hovering status (in Watt-hour) can be calculated by[4]

$$E_{\text{out}} = P_{\text{out}}T, \quad (8)$$

where P_{out} is the required power for the UAV to maintain aloft. It is given by [23], [24]

$$P_{\text{out}} = \frac{1}{\eta_{\text{rotor}}} \sqrt{\left(\frac{2W^3}{\rho A}\right)}, \quad (9)$$

where η_{rotor} is the rotor's efficiency and A denotes the rotor disc area. In (9), W denotes the weight force and is given by $W = mg$ where m is the mass of the UAV and g is the gravitational acceleration. In (9), ρ denotes air density and is given by [25]

$$\rho = \frac{p_0 \mu}{\varpi t_0} \left(1 - \frac{\sigma h}{t_0}\right)^{\frac{g\mu}{\varpi\sigma} - 1}, \quad (10)$$

where p_0 is sea level standard atmospheric pressure, μ is molar mass of dry air, ϖ is ideal gas constant, t_0 is sea level standard temperature, and σ is temperature lapse rate.

[3]Solar noon is the moment when the Sun reaches its highest position in the sky which is typically observed at 12:00 pm.

[4]For most practical purposes, payload energy consumption (which includes avionics and communication system power consumption) can be considered negligible.

III. OPTIMIZATION OF UAV OPERATION ALTITUDE

In this section, we formulate an optimization problem to determine the UAV operation altitude. We aim to maximize the net energy defined as

$$E_{\text{net}} = E_{\text{in}} - E_{\text{out}}. \quad (11)$$

The optimization is carried out under the constraints of achieving an acceptable probability of LOS while respecting the aerodynamic specifications of the UAV which imposes a maximum operation altitude for the UAV. Mathematically speaking, we have

$$\begin{aligned} h_{\text{opt}} = \arg\max_h \ & E_{\text{net}} \\ \text{s.t.} \quad \text{C1}: \ & P_{\text{LOS}} > P_{\text{LOS,th}} \\ \text{C2}: \ & h \leqslant h_{\text{max}} \end{aligned} \quad (12)$$

The constraint C1 imposes a minimum required altitude for the UAV to satisfy a targeted acceptable probability of LOS denoted by $P_{\text{LOS,th}}$. The minimum operation altitude (i.e., h_{min}) to achieve this is obtained by numerically solving (1) for h. Constraint C2 imposes a maximum operation altitude for the rotary-wing UAV (i.e., $h \leqslant h_{\text{max}}$) dictated by the UAV aerodynamic design.

It can be readily checked that the second derivative of E_{net} with respect to the altitude gives negative values for practical values of the altitude. Therefore, the function is concave, and it always has one single optimum solution which we aim to obtain in the following. Replacing (7) and (8) in (11), we obtain E_{net} as

$$\begin{aligned} E_{\text{net}} = & E_{\text{b}} + \frac{E_{\text{h}}}{\psi}\left(0.8978 - 0.2804\exp\left(-\frac{h}{3500}\right)\right) \\ & - \frac{\left(2\varpi t_0 W^3\right)^{\frac{1}{2}}T}{\left(A p_0 \mu\right)^{\frac{1}{2}}\eta_{\text{rotor}}} t_0^{0.5\left(\frac{g\mu}{\varpi\sigma}-1\right)}(t_0 - \sigma h)^{-0.5\left(\frac{g\mu}{\varpi\sigma}-1\right)}. \end{aligned}$$
$$(13)$$

We take the derivative of (13) with respect to the altitude and set the resulting expression to zero. Under the assumption of $\sigma h \ll t_0$ (which can be justified for low altitude UAVs[5]), the optimum altitude can be obtained as

$$h_{\text{opt}} \approx -3500 \ln\left(\frac{6241\psi\sigma\left(\frac{g\mu}{\varpi\sigma}-1\right)T\sqrt{\left(\frac{2\varpi t_0 W^3}{A p_0 \mu}\right)}}{E_{\text{h}} t_0 \eta_{\text{rotor}}}\right). \quad (14)$$

The above solution was obtained without taking into account the constraints of C1 and C2. Recall that these constraints basically dictate the minimum and maximum values allowed for the operation altitude. If h_{opt} calculated from (14) is within the allowable range of $h_{\text{min}} \leq h_{\text{opt}} \leq h_{\text{max}}$, h_{opt} is indeed the optimum altitude. If h_{opt} is lower than the minimum altitude imposed by constraint C1, h_{min} becomes the optimum solution, i.e., $h_{\text{opt}} = h_{\text{min}}$. On the other hand, if h_{opt} is higher than the maximum altitude imposed by constraint C2, h_{max} becomes the optimum solution, i.e., $h_{\text{opt}} = h_{\text{max}}$.

[5]In numerical results, the maximum altitude is considered to be 3 km.

$$E_{\text{h}} = \frac{180\tau\psi A_{\text{s}}\eta_{\text{sc}}G_{\text{m}}}{\xi_{\text{m}}\pi}\left[\cos\left(\frac{2\xi_{\text{m}}}{\tau}(12 - t_{\text{sunset}})\right)\left(\cos\left(\frac{\xi_{\text{m}}}{\tau}T\right) - 1\right) + \sin\left(\frac{2\xi_{\text{m}}}{\tau}(12 - t_{\text{sunrise}})\right)\sin\left(\frac{\xi_{\text{m}}}{\tau}T\right)\right]. \quad (6)$$

TABLE I

SPECIFICATIONS OF THE SOLAR-POWERED ROTARY-WING UAV

Parameter	Variable	Value
Total Mass of the UAV	m (kg)	8
Solar Area	A_s (m^2)	4
Rotor Disk Area	A (m^2)	0.503
Acceleration	g (m/s^2)	9.8
Solar Constant	G_{sc} (W/m^2)	1366.1
Efficiency of the Solar Cell	η_{sc}	37.5 (%)
Horizontal Distance between the UAV and Base Station	D (m)	1000
Height of Base Station	h_{BS} (m)	50
Maximum Altitude of the UAV	h_{max} (m)	3000
Rotor's Efficiency	η_{rotor}	90 (%)
The initial battery capacity	E_b (Wh)	500 [26]

TABLE II

AIR DENSITY VARIABLES

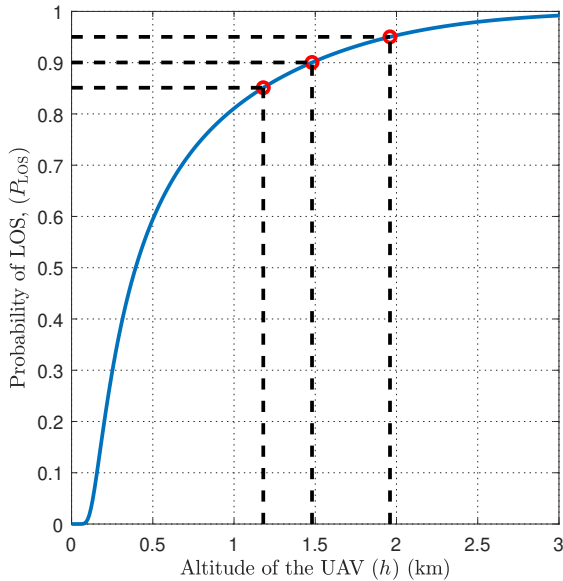| Parameter	Variable	Value
Sea Level Standard Atmospheric pressure	p_0 (J/m^3)	101325
Molar Mass of Dry Air	μ (kg/mol)	0.0289
Ideal Gas Constant	ϖ (J/mol.K)	8.3144
Sea Level Standard Temperature	t_0 (K)	288.15
Temperature Lapse Rate	σ (K/m)	0.0069

Fig. 3. Probability of LOS with respect to the altitude of the UAV

IV. NUMERICAL RESULTS

In this section, we present numerical results to demonstrate the benefits of optimization of the UAV operation altitude as well as discuss the effect of various system parameters on this optimization. The amount of harvested energy by the solar-powered UAV is obviously dependent on the time of the day and the geographical location. To assess the energy harvested by the UAV, we consider Ankara, Turkey with latitude of $L = 39.86°$, and $d = 150^{th}$ day of the year. We assume a Gallium Arsenide (GaAs) solar panel with an efficiency of $\eta_{sc} = 37.5\%$ [27] and a battery capacity of $E_b = 500$ Wh.
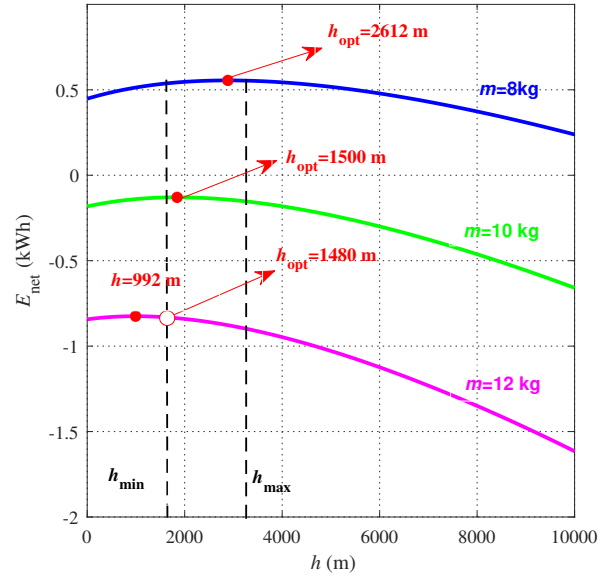

Fig. 4. Net energy with respect to altitude for rotary-wing UAVs with different weights.

Unless otherwise stated, the UAV specifications in Table I are used in our study. The air density variables for the calculation of (10) are provided in Table II.

In Fig. 3, we present the probability of LOS with respect to different altitudes of the UAV to determine the minimum allowable altitude. We assume an urban areas with the ratio of built-up area to the total area $\alpha = 0.4$, the average number of buildings per km^2, $\beta = 1000$, and the mean building's heights $\mu_H = 50$ m. Based on (1), for the given parameters, if the targeted probability of LOS is set as $P_{LOS,th} = 0.95$, the required minimum altitude is found as $h_{min} = 1960$ m. For $P_{LOS,th} = 0.9$ and 0.85, the minimum altitude reduces to respectively $h_{min} = 1480$ m, and $h_{min} = 1180$ m. It is obvious that the higher the operation altitude of the UAV, the higher the probability of establishing an unobstructed link with base stations. In the following, we use $P_{LOS,th} = 0.9$ which is reasonably high for most practical cases.

In Fig. 4, we present the net energy with respect to altitude for various UAV weights based on (13) assuming an airborne time of $T = 1$ hour. As discussed above, the minimum altitude is dictated by the LOS requirements and given by $h_{min} = 1480$ m for the scenario under consideration. The maximum allowable operation altitude is related to the aerodynamic specifications of the UAV. It is dependent on its weight, type of motors, propulsion configurations, and type of battery. For typical rotary-wing UAVs, the maximum altitude is around $h_{max} = 3000$ m [28]. Therefore, we need to stay within the range of 1480 m up to 3000 m, (shown in dashed vertical lines in Fig. 4). In Fig. 4, we consider a wider range of altitudes between $h = 0$ m and $h = 10000$ m to demonstrate that the net energy is indeed a concave function. It is observed that there is always one point (shown in red) that maximizes the net energy. From (14), the optimum altitudes are respectively obtained as $h = 2612$m, $h = 1500$m, and $h = 992$m, for the UAV weights of $m = 8$ kg, $m = 10$ kg, and $m = 12$ kg. It can be readily checked that all these values are higher than the minimum allowable altitude and lower than the maximum
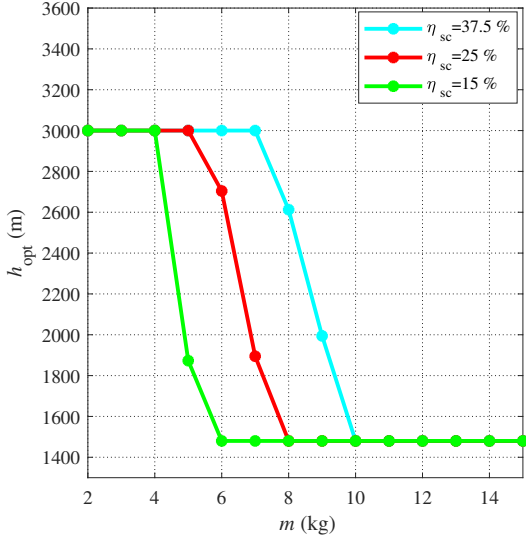
Fig. 5. Optimum altitude versus UAV weight for different values of solar panel efficiency.

Fig. 6. Optimum altitude versus solar panel size for different values of solar panel efficiency.

altitude of 3000 m. However, for $m = 12\,\text{kg}$, the optimal value determined from (14) is $h = 992\,\text{m}$ which is lower than the minimum altitude. Therefore, the minimum altitude imposed by LOS constraints, $h = 1480\,\text{m}$ should be selected as the operation altitude.

In Fig. 5, we present the optimal altitude with respect to the UAV's weight. We consider a solar panel with a surface area of $A_s = 4\,\text{m}^2$ and assume different solar efficiencies of $\eta_{sc} = 37.5\%$, $\eta_{sc} = 25\%$, and $\eta_{sc} = 15\%$. It can be observed that the optimal altitude decreases as the solar efficiency decreases for a fixed weight. For example, consider a solar-powered UAV with a weight of $m = 8\,\text{kg}$. While its optimum altitude is $h = 2612\,\text{m}$ for $\eta_{sc} = 37.5\%$, it decreases to $h = 1480\,\text{m}$ for $\eta_{sc} = 25\%$, and $\eta_{sc} = 15\%$. The optimal value from (14) for $\eta_{sc} = 25\%$, and $\eta_{sc} = 15\%$ is actually lower and given by $h = 1193\,\text{m}$, and $h = 13\,\text{m}$, respectively. Here, the minimum altitude dictated by the LOS requirement is used. Similarly, for $\eta_{sc} = 25\%$, the optimum altitude for the UAVs for weights larger than $m = 8\,\text{kg}$ is determined by this minimum altitude and hence given by $h = 1480\,\text{m}$. For $\eta_{sc} = 15\%$, the minimum altitude becomes the optimal altitude for UAVs for weights higher than $m = 6\,\text{kg}$.

In Fig. 6, we present the optimal altitude with respect to the solar panel area. We consider an UAV with a weight of $m = 8\,\text{kg}$ and assume different solar efficiencies of $\eta_{sc} = 37.5\%$, $\eta_{sc} = 25\%$, and $\eta_{sc} = 15\%$. It is observed that the optimum altitude increases as the solar surface area increases for a fixed value of solar efficiency[6]. For example, assume that UAV is equipped with a solar panel having a solar efficiency of $\eta_{sc} = 25\%$, The optimum altitude for the solar panel size of $A_s = 4\,\text{m}^2$ is $h = 1480\,\text{m}$. This increases to $h = 2612\,\text{m}$ for $A_s = 6\,\text{m}^2$.

---

[6]GaAs solar panels weigh approximately 200g per meter square [27]. The extra weight will affect the overall weight of the UAV and consequently result in an increase in the energy consumption. This issue was taken into account in our calculations.
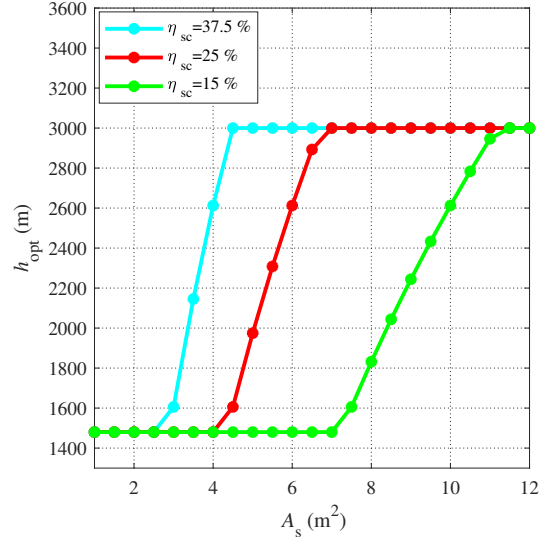
V. Conclusion

In this paper, we investigated the optimal selection of the operation altitude of a solar-powered rotary-wing UAV which provides FSO backhauling to a ground base station. The optimal altitude was determined to maximize the net energy under the constraints of achieving an acceptable probability of LOS (which dictates the minimum allowable altitude) and respecting the aerodynamic specifications of the UAV (which imposes a maximum operation altitude). Our results have shown that the optimized value of operation altitude is highly dependent on UAV's weight as well as the size and efficiency of the solar panel. Specifically, the optimal altitude decreases as the solar efficiency decreases for a fixed weight. On the other hand, it increases as the solar surface area increases for a fixed value of solar efficiency. Judiciously selected operation altitude has the potential to significantly enhance the airborne time of UAV as a result of energy optimization.

Appendix

In this Appendix, we calculate the maximum instantaneous radiation intensity at solar noon, i.e., G_m, which is required for the calculation of (4). The maximum instantaneous radiation intensity at solar noon is given by [21]

$$
\begin{aligned}
G_m = G_{sc} & \left(1 + 0.033 \cos\left(\frac{360d}{365}\right)\right) \\
& \times \left(\sin\left(\xi_m + \delta\right) \cos\left(\delta\right) - \cos\left(\xi_m + \delta\right) \sin\left(\delta\right)\right),
\end{aligned}
\tag{15}
$$

where G_{sc} is solar constant, d is the specific day of the year (represented by a value between 1 and 365), δ is the solar declination angle, and ξ_m is the maximum elevation angle of the sun. The maximum elevation angle of the sun depends on the latitude of the location of interest L, and varies with day of the year. It is given by $\xi_m = 90° + L - \delta$. The solar declination angle represents the angle between the line joining the centres of the sun and the earth and its projection on the equatorial plane and is given by [21]

$$
\delta = -23.45 \cos\left(\frac{360}{365}\left(10 + d\right)\right).
\tag{16}
$$

REFERENCES

[1] N. Elmeseiry, N. Alshaer, and T. Ismail, "A detailed survey and future directions of unmanned aerial vehicles (UAVs) with potential applications," *Aerospace*, vol. 8, no. 12, 2021.

[2] M. Mozaffari, W. Saad, M. Bennis, Y.-H. Nam, and M. Debbah, "A tutorial on UAVs for wireless networks: Applications, challenges, and open problems," *IEEE Commun. Surv. Tutor.*, vol. 21, no. 3, pp. 2334–2360, 2019.

[3] C. Zhang, L. Zhang, L. Zhu, T. Zhang, Z. Xiao, and X.-G. Xia, "3D deployment of multiple UAV-mounted base stations for UAV communications," *IEEE Trans. Commun.*, vol. 69, no. 4, pp. 2473–2488, 2021.

[4] J. Lyu, Y. Zeng, R. Zhang, and T. J. Lim, "Placement optimization of UAV-mounted mobile base stations," *IEEE Commun. Lett*, vol. 21, no. 3, pp. 604–607, 2017.

[5] Y. Zeng, X. Xu, and R. Zhang, "Trajectory design for completion time minimization in UAV-enabled multicasting," *IEEE Trans Wireless Commun.*, vol. 17, no. 4, pp. 2233–2246, 2018.

[6] P. Yang, X. Cao, X. Xi, W. Du, Z. Xiao, and D. Wu, "Three-dimensional continuous movement control of drone cells for energy-efficient communication coverage," *EEE Trans. Veh. Technol.*, vol. 68, no. 7, pp. 6535–6546, 2019.

[7] J.-H. Lee, K.-H. Park, Y.-C. Ko, and M.-S. Alouini, "Spectral-efficient network design for high-altitude platform station networks with mixed RF/FSO system," *IEEE Trans Wireless Commun.*, vol. 21, no. 9, pp. 7072–7087, 2022.

[8] M. Ke, Z. Gao, Y. Huang, G. Ding, D. W. K. Ng, Q. Wu, and J. Zhang, "An edge computing paradigm for massive IoT connectivity over high-altitude platform networks," *IEEE Wireless Commun.*, vol. 28, no. 5, pp. 102–109, 2021.

[9] M. Alzenad, M. Z. Shakir, H. Yanikomeroglu, and M.-S. Alouini, "FSO-based vertical backhaul/fronthaul framework for 5G+ wireless networks," *IEEE Commun. Mag.*, vol. 56, no. 1, pp. 218–224, 2018.

[10] Y. Sun, D. Xu, D. W. K. Ng, L. Dai, and R. Schober, "Optimal 3D-trajectory design and resource allocation for solar-powered UAV communication systems," *IEEE Trans. Commun.*, vol. 67, no. 6, pp. 4281–4298, 2019.

[11] A. Al-Hourani, S. Kandeepan, and S. Lardner, "Optimal LAP altitude for maximum coverage," *IEEE Commun. Lett.*, vol. 3, no. 6, pp. 569–572, 2014.

[12] S. Sekander, H. Tabassum, and E. Hossain, "Statistical performance modeling of solar and wind-powered UAV communications," *IEEE Trans. Mob. Comput.*, vol. 20, no. 8, pp. 2686–2700, 2021.

[13] Y. Zhou, Z. Gu, J. Zhang, and Y. Ji, "Efficient deployment of aerial relays in FSO-based backhaul networks," *J. Opt. Commun. Netw.*, vol. 15, no. 1, pp. 29–42, 2023.

[14] Y. L. Che, W. Long, S. Luo, K. Wu, and R. Zhang, "Energy-efficient UAV multicasting with simultaneous FSO backhaul and power transfer," *IEEE Commun. Lett.*, vol. 10, no. 7, pp. 1537–1541, 2021.

[15] M. T. Dabiri, M. Rezaee, L. Mohammadi, F. Javaherian, V. Yazdanian, M. O. Hasna, and M. Uysal, "Modulating retroreflector based free space optical link for UAV-to-ground communications," *IEEE Trans. Wireless Commun.*, vol. 21, no. 10, pp. 8631–8645, 2022.

[16] S. Janji, A. Samorzewski, M. Wasilewska, and A. Kliks, "On the placement and sustainability of drone FSO backhaul relays," *IEEE Commun. Lett.*, vol. 11, no. 8, pp. 1723–1727, 2022.

[17] B. Tezergil and E. Onur, "Wireless backhaul in 5G and beyond: Issues, challenges and opportunities," *IEEE Commun. Surv. Tutor.*, vol. 24, no. 4, pp. 2579–2632, 2022.

[18] P. Bhardwaj and S. M. Zafaruddin, "Performance of dual-hop relaying for THz-RF wireless link over asymmetrical α-μ fading," *EEE Trans. Veh. Technol.*, vol. 70, no. 10, pp. 10 031–10 047, 2021.

[19] M. M. Azari, F. Rosas, K.-C. Chen, and S. Pollin, "Optimal UAV positioning for terrestrial-aerial communication in presence of fading," in *2016 IEEE Global Communications Conference (GLOBECOM)*, 2016, pp. 1–7.

[20] R. Series, "Propagation data and prediction methods required for the design of terrestrial line-of-sight systems," *Recommendation ITU-R*, pp. 530–12, 2015.

[21] S. C. Arum, D. Grace, P. D. Mitchell, M. D. Zakaria, and N. Morozs, "Energy management of solar-powered aircraft-based high altitude platform for wireless communications," *Electronics*, vol. 9, no. 1, 2020.

[22] J.-S. Lee and K.-H. Yu, "Optimal path planning of solar-powered UAV using gravitational potential energy," *IEEE Trans. Aerosp. Electron. Syst.*, vol. 53, no. 3, pp. 1442–1451, 2017.

[23] A. Klesh and P. Kabamba, "Energy-optimal path planning for solar-powered aircraft in level flight," in *AIAA guidance, navigation and control conference and exhibit*, 2007, p. 6655.

[24] H. V. Abeywickrama, B. A. Jayawickrama, Y. He, and E. Dutkiewicz, "Comprehensive energy consumption model for unmanned aerial vehicles, based on empirical studies of battery performance," *IEEE Access*, vol. 6, pp. 58 383–58 394, 2018.

[25] C. Peng, J. Wang, and D. Wu, "Impacts of air density fluctuations toward the mass measurements of a 1 kg silicon sphere," *IEEE Access*, vol. 8, pp. 140 840–140 847, 2020.

[26] https://www.aeroexpo.online/prod/challenger-aerospace-systems/product 1869476845.html [accessed january 22, 2023].

[27] https://www.alibaba.com/product-detail/gallium-arsenide-solar-cells [accessed january 23, 2023].

[28] https://www.aeroexpo.online/prod/slidx/product-175273-15858.html [accessed june 30, 2022].